

Thermodynamic simulation and pinch analysis of KCS₁₁

Authors

Ali Behbahani-nia^{a*}
Rasool Bahrapouri^a

^a Department of Mechanical Engineering, K.N. Toosi university of technology, Mollasadra St., Tehran, Iran

ABSTRACT

In this study, a reputable Kalina cycle system, KCS 11, is simulated and analysed. Within this efficient cycle, there are three heat exchangers: the first heat exchanger is designated for heat absorption from the heat source, the second heat exchanger is designed for heat release to the cold source, and the third heat exchanger is designed for energy recovery. In order to achieve precise simulation, a variation of heat capacity is considered. A finite difference method is, therefore, implemented in consideration of the amount of heat transfer in each heat exchanger. In this study, combustion exhaust is considered as the heat source, while cooling water circulates in the condenser. The effect of the product of the overall heat transfer coefficient and the heat transfer area on decisive parameters including the net power output and the efficiency is investigated. Moreover, the influences of the studied parameters are examined on two important pinch technology related curves; these are: the composite curve and the grand composite curve. The results indicated that although increasing the heat transfer surface in each of the heat exchangers boosts the power output, in some cases, it reduces the cycle's efficiency.

Article history:

Received : 4 October 2016

Accepted : 28 December 2016

Keywords: Kalina Cycle, Heat exchanger, Thermodynamic, Pinch Analysis.

1. Introduction

The goal of systems thermal efficiency improvement has always been targeted by researchers in order to reduce energy consumption. It is clear that this issue requires extra attention when a large amount of energy is produced; therefore, power plants are always being improved throughout the recent century. In order to increase the efficiency of the traditional power plant in which water circulates as the heat transfer fluid, Kalina introduced a cycle [1]. The presented cycle is not only attractive for its high efficiency, but also its ability to work with low temperature heat sources [2]. Different types of the Kalina cycle have been introduced thereafter, for

which a brief collection was prepared by Zhang et al. [3].

Yet, diverse comparisons between different KCSs (Kalina Cycle Systems) and ORCs (Organic Rankine Cycles) have been carried out. The effect of implementation of an ejector instead of the traditionally employed pressure valve has been studied by Li et al. [4]. The comparison of the idea generated cycle and the KCS 11 revealed that the novel cycle generates extra power more efficiently. The effect of the substitution of the pressure valve by two phase expanders is studied in two different arrangements and a comparison among the three cycles is performed [5]. It has been concluded that the implementation of the expander in a special configuration leads to efficiency promotion to 27 percent. The comparisons of the KCS with the similar ORC as well as a supercritical ORC beside the TLC are also carried out [6 and 7].

In addition, KCS 11 has been coupled with different heat sources including geothermal

*Corresponding author: Ali Behbahani-nia
Address: Department of Mechanical Engineering, K.N. Toosi university of technology, Mollasadra St., Tehran, Iran
E-mail address: alibehbahani@kntu.ac.ir

[8] and solar [9 and 10] heat sources. Mlack [8] showed that KCS 11 works most effectively with low temperature heat sources between 250 and 400 °C. Sun et al. studied the effect of reheating the mixture stream heated by a solar source to a supercritical condition via an auxiliary energy system [9].

Wang et al. investigated the effect of the different parameters of KCS 11, driven by a parabolic collector [10]. They recognized the most effective parameters of the cycle performance and optimized it by varying the selected parameters. Wang et al. showed that the turbine inlet pressure strongly affects the amount of the generated power, while the stream temperature has a much smaller influence on the decisive parameters. Ogriseck examined a couple of the KCS and a combined cycle power plant in order to recover the plant's exhaust heat [11]. In the study, the upper pressure of the cycle and the ammonia mass fraction were explored under five different conditions. His results showed that the integrated cycle's efficiency may grow up to 17 percent. This cycle's integration with a coal power plant was also studied [12]. The exergetic efficiency of the integrated cycle was examined for varying mass fractions of ammonia and the cycle's pressure. Results showed that the selection of optimum values improved the energetic efficiency of the cycle up to 27 percent. Yue et al. considered the exhaust of an internal engine as the heat source of the KCS [6]. They reported that within a special temperature range, an ORC exhibits some advantages over the KCS 11.

In order to evaluate energy systems, pinch analysis has been introduced across a diverse range of applications; these include the study of a gas turbine [13], a methanol plant [14], a geothermal driven heat pump [15], combined heat and power [16], and a steam power plant [17]. The evaluation of pinch specifications involving pinch temperature is much more complicated for systems that involve water-ammonia due to its varying thermal capacity during heat absorption. A method for the evaluation of the pinch temperature difference has been proposed for a single heat exchanger (evaporator or condenser) [18]. The results demonstrate that the pinch temperature is a strong function of ammonia concentration and working pressure. Owing to the aforementioned complexity, only a small number of studies include pinch analysis. Sun et al. simulated a KCS in which the regenerator's pinch temperature difference was set to 5 °C [9]. Peng et al. considered a

coupled-intercooled gas turbine and a KCS that was integrated with a solar system, which was studied via the consideration of certain energy related curves.

In this paper, the KCS 11 was investigated thermodynamically and a pinch analysis was presented to clarify the thermal performance of the system. This study focuses on each of the heat exchangers included in the cycle in order to explain the behaviour of the system when the heat transfer area expands. In some previous studies, the pinch temperature was assumed to be reached at each of the heat exchangers' ends [4 and 10], whereas in some others, one of the outlet temperatures or the heat exchangers' efficiency was considered constant [5 and 7]. Owing to the nonlinear temperature–enthalpy curve of the mixture, in some conditions the assumption of pinch occurrence at either ends of the heat exchangers introduces large approximations [18]. In the current study, the heat exchangers are studied via the implementation of the finite difference method, which is justified when at least one of the heat exchangers' streams behave nonlinearly during heat absorption [19]. The implementation of this method enables the possibility of the exact simulation of the heat exchangers, which results in a more realistic outcome. As long as the KCS's working fluid operates nonlinearly when it absorbs or releases heat, the composite curve and the grand composite curve must be plotted by a method other than the classical methods, in which thermal capacity is considered constant. In this paper, the pinch-related curves are plotted using numerous points for each of the streams existing in the heat exchanger.

Nomenclature

$A(m^2)$	heat transfer area
$h(kJ/kg)$	enthalpy
$\dot{Q}(kW)$	heat transfer rate
$\dot{m}(kg/s)$	mass flow rate
n	number of sections
$P(bar)$	pressure
$T(K)$	temperature
$U(kW/(m^2K))$	overall heat transfer coefficient
v	stream velocity
$z(m)$	altitude

Subscript

bs	basic stream
c	cold stream
con	condenser
e	exit

eva	evaporator
h	hot stream
htf	heat transfer fluid
flue	flue gas
i	inlet
reg	regenerator

2. Pinch Analysis

In order to analyse a system by using pinch technology, some streams are considered as cold and some are considered hot streams. Pinch analysis, which is basically a graphical technique, was first introduced by B. Linnhoff and V. Sahdev, in which heat capacity of all streams were considered constant [20].

As observable in Fig.1(a), there are two hot streams, both of which lose their temperatures. The algorithm introduced by pinch technology is depicted in Fig.1(b). Comparing both figures, one can conclude that the temperature axis has been divided into three sections: 40–80, 80–130, and 130–180. In the first and the last intervals, only one stream exists; therefore, in the corresponding interval of the composite curve, a similar line with the same slope is observable. On the other hand, the 80–130 interval contains both the lines in Fig.1(a). In order to construct the composite curve in this interval, the thermal capacities of the two streams are added to play the same role in heat rejection as well as thermal variation.

It is clear that the explained method of constructing the composite curve is based on constant heat capacity. A question may arise regarding the outcome of the streams' heat capacity variance during heat absorption. The solution to this question is that the temperature values of the streams during heat rejection have to be implemented.

It is clear that the true implementation of the technique depends on the amount of heat capacity, which varies during heat transfer. Since the water–ammonia mixture temperature does not behave linearly, especially during phase change [18], the consideration of constant heat capacity is occasionally unreasonable. In order to draw the pinch-related curves of the heat exchanger network of KCS 11, therefore, a new method is introduced, in which, instead of thermal capacities, point by point thermal values of the streams should be known. The integrated cold stream, which was previously formed by the inlet and outlet temperatures and the thermal capacity of the streams, is now built by an iterative summation of enthalpy values for every temperature within a temperature range. A detailed procedure of this method is presented in Fig.2. As the algorithm to draw a composite curve for cold streams is similar to that of hot streams, the procedure that is given as a flowchart can be applied for both streams.

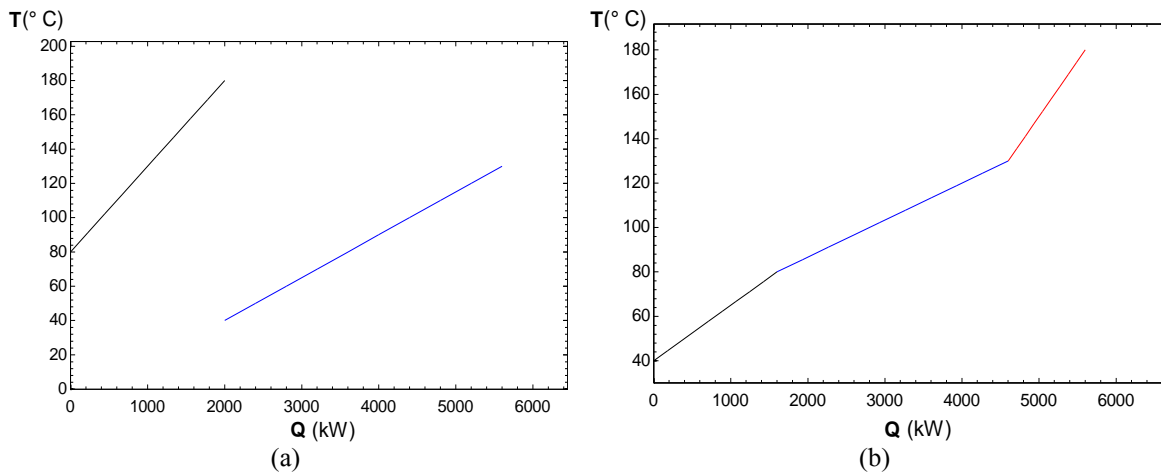


Fig.1. Temperature versus heat (a) stream lines and (b) the composite curve

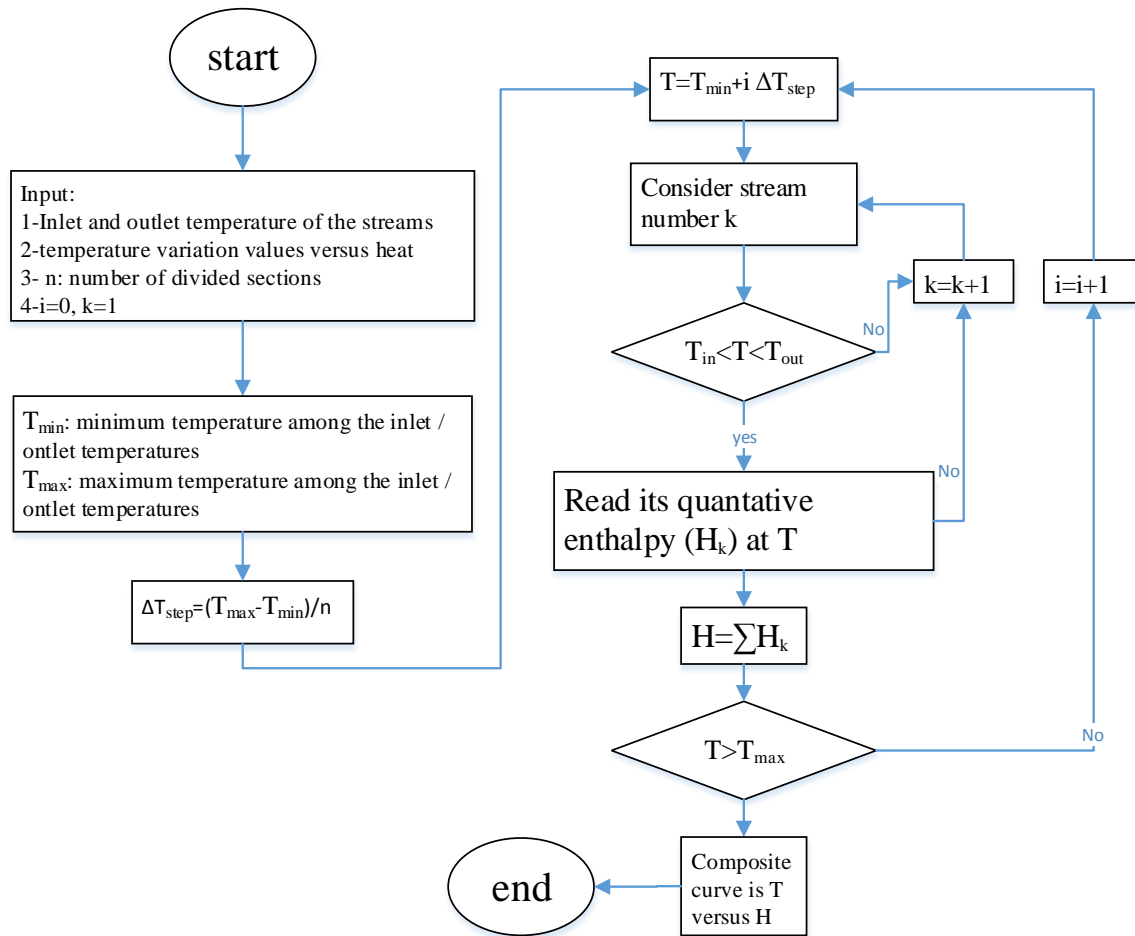


Fig.2. The flowchart of the pinch analysis for varying heat capacity

3. System Definition

As mentioned previously, the KCS is more capable in founding a match with heat sources due to its varying temperature during phase change; therefore, the efficiency of the KCS is greater than the similar ORCs [21]. Certain types of this cycle are designed to match high temperature heat sources, whereas others are well coupled with low temperature sources. Among these, the KCS 11, which is considered to operate acceptably with moderate and low temperature heat sources, has attracted considerable attention for its simplicity and high efficiency. As shown in Fig.3(a), a cycle's stream (10) absorbs some heat and leaves the evaporator as it contains both liquid and vapour phases (1). Therefore, the phases can be split up in a separator from which the ammonia-rich vapour can flow into

the turbine (2). The remaining liquid extract (3), in which a lesser concentration of ammonia exists, preheats the supply stream. The weak stream thereafter enters the pressure valve (5) which results in a pressure drop in the stream. The weak stream (6) is now prepared to be mixed with the turbine's exhaust (4); the resultant product (7) condenses in a condenser. The condensate (8) is then pumped (9) to be preheated (10) by the aforementioned liquid extract of the separator.

The illustrated thick lines in Fig.3(a) exhibit the higher pressure parts of the cycle. Figure 3(b) shows each of the aforementioned points of the cycle by a point in the enthalpy–ammonia mass fraction graph. For further clarification, the filled points are designated to the high-pressure sections of the cycle and the hollow points are related to the low-pressure parts.

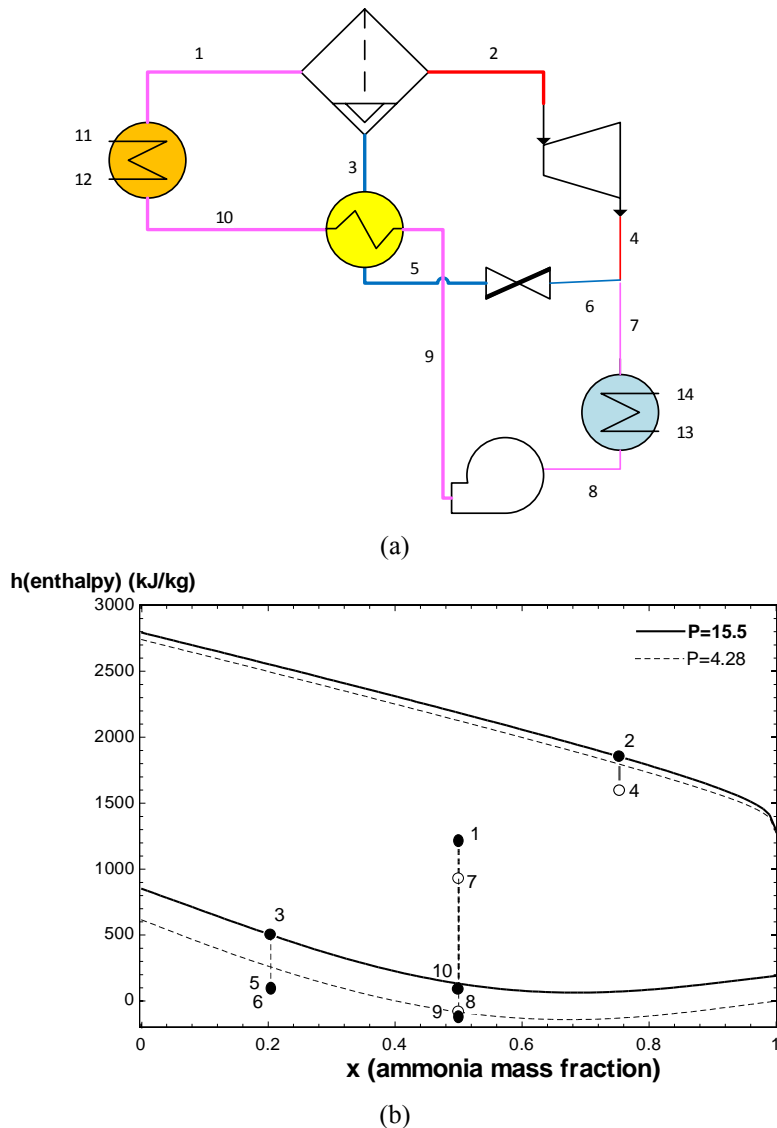


Fig.3. (a) A schematic view of the KCS 11 and (b) the cycle’s streams in the enthalpy–ammonia mass fraction coordinates

3.1. Mathematical model

In this study, the evaluation of the properties of the ammonia–water mixture are carried out by employing the relations proposed by Ibrahim and Klein [22]. The simulation of the cycle is developed to consider the heat transfer area consequences (UA) as an input.

During the simulation, the following assumptions are made:

- The temperature of the water inlet to the condenser is 15°C.
- The pressure drop within the connecting pipes, the fittings, and the heat exchangers are negligible.
- The isentropic efficiency of the pressure changing components (turbine and pump) are equal to 1.

- UA is assumed to remain constant during simulation.

One of the main features of the present paper is the last assumption. In fact, as pressure and water–ammonia concentration may vary during sensitivity analysis or optimization, and since these parameters alter the streams’ enthalpy–temperature curve, the occurred pinch temperature difference may vary from the specified difference throughout the analysis. The assumption of the UA remaining constant, therefore, seems to be much more realistic, although it ensures a complicated analysis and a far greater CPU cost.

3.2. Cycle simulation

Unlike previous investigations, UA has been regarded as an input for the currently modelled cycle. The cycle's simulation algorithm, in which UA is an input, is shown in Fig.4. The corresponding details for the inclusion of the consequences of the streams' heat capacity variation are introduced in the following section.

The introduced KCS, in addition to the heat exchangers, employs different components including a separator, a turbine, a pressure valve, and a pump. In order to specify the thermodynamic properties at the inlet(s) or the outlet(s) as well as the amount of transferred energy, the energy and the mass conservation equations, Eq.(1) and Eq. (2), should be solved.

$$\dot{Q} = \dot{W} + \sum \dot{m}_e (h_e + \frac{v_e^2}{2} + gz_e) - \sum \dot{m}_i (h_i + \frac{v_i^2}{2} + gz_i) \quad (1)$$

$$\sum \dot{m}_i = \sum \dot{m}_e \quad (2)$$

3.2.1. The Modelling of the Heat Exchangers

In this study, the heat exchangers, including the evaporator, the condenser, and the regenerator, are modelled via an implementation of the finite difference method. With respect to Fig.5, the amount of transferred heat within each of the finite sections can be calculated using Eq.(3):

$$\delta Q = \frac{Q}{n} \quad (3)$$

where n is the number of sections that the heat exchanger is divided into. It is clear that the greater the number of divisions, the more accurate the simulation will be. In this study, this number is selected to be 100 for each of the heat exchangers.

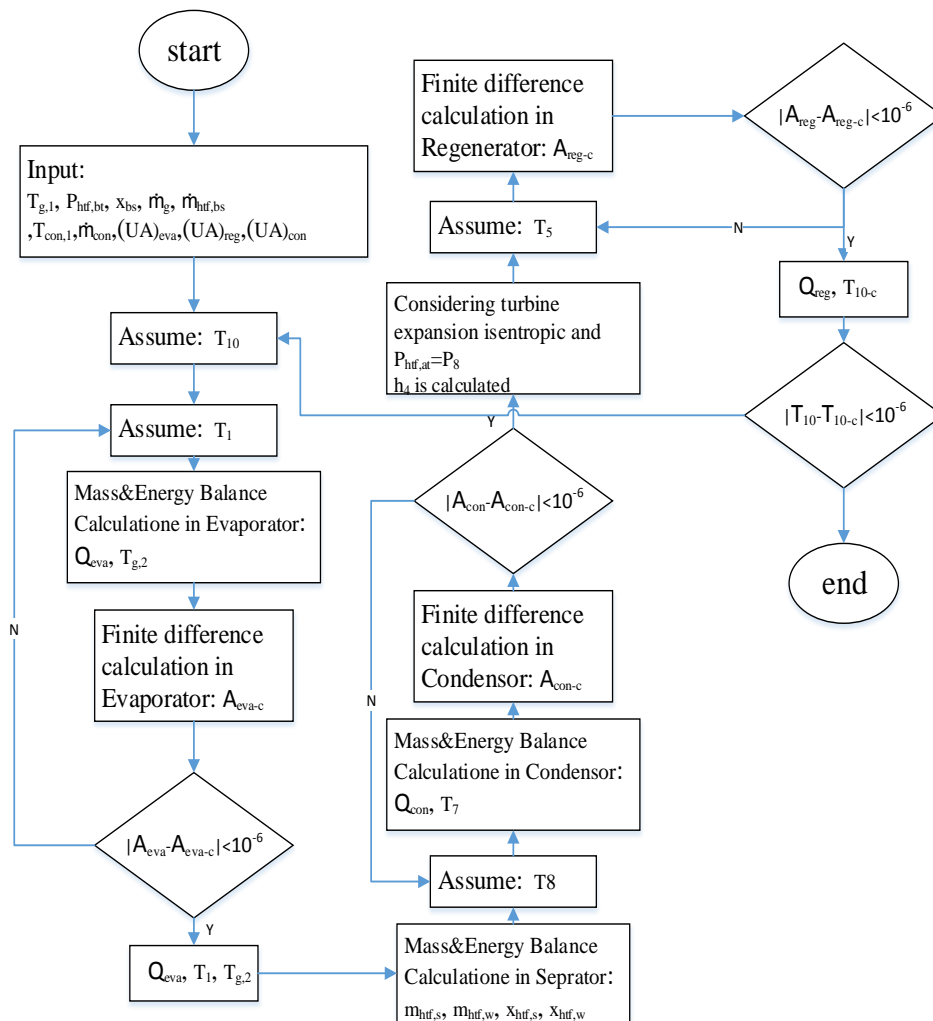


Fig.4. The flowchart of the simulation process details of the KCS

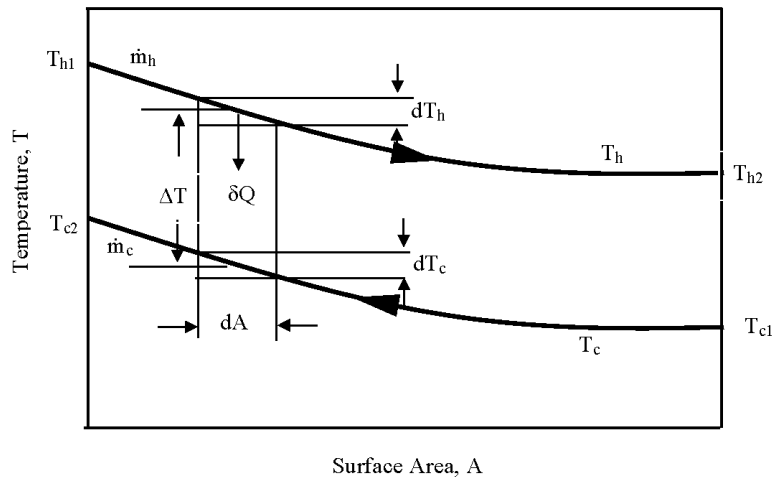


Fig.5. Temperature versus area along the heat exchanger

Within each of these sections, owing to the small amount of the divided heat, the temperature variation can be considered negligible. Therefore, the following equations hold:

$$\delta Q = U(T_h - T_c)dA \tag{4}$$

A summation of the UdA s gives the total UA for the heat exchanger:

$$UA = \sum_{i=0}^n \frac{\delta Q}{(T_{h,i} - T_{c,i})} \tag{5}$$

where $T_{h,i}$ and $T_{c,i}$ are the varying hot and cold temperatures within the heat exchanger for the i^{th} section. Figure 4 shows the temperature profile of a counter flow heat exchanger versus area. In this figure, the sections and its related parameters are illustrated.

In this study, for each of the heat exchangers, UA has been considered as an input. The calculation process requires an iterative trial-and-error method in order to obtain the unknown heat exchanger outlet.

4.Validation

The validation of this paper’s result is designated to the method introduced for pinch analysis and its resulting composite curve. As pinch analysis is a graphical tool for the thermal condition of the system, a comparison between the stream lines and their corresponding composite curve can be considered as the validation of the method.

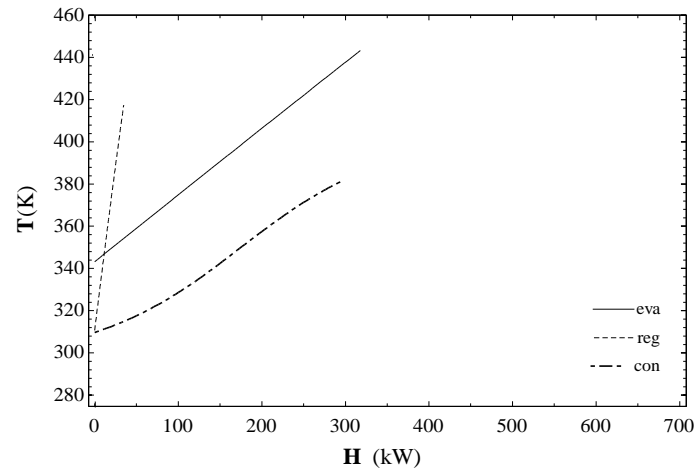
Figure 6a shows the temperature–enthalpy variation for the hot streams of the three heat

exchangers. Figure 6(b) illustrates the corresponding composite curve, which is the outcome of the explained algorithm presented in Section 2. A comparison between these two implies that the total amount of heat release for the three streams equals that of the composite curve. Moreover, the trend of composite curve variation ascertains that the rules presented in the classical pinch analysis for constructing a composite curve hold. For example, in the composite curve given in Fig.6(b), as the temperature exceeds 340°C, the slope of the curve reduces; this corresponds to the emergence of the evaporator’s stream line as shown in Fig.6(a). As the values for heat capacity are supposed to be added in the same temperature interval, the reduction in the slope verifies the increase in the heat capacity above 340°C.

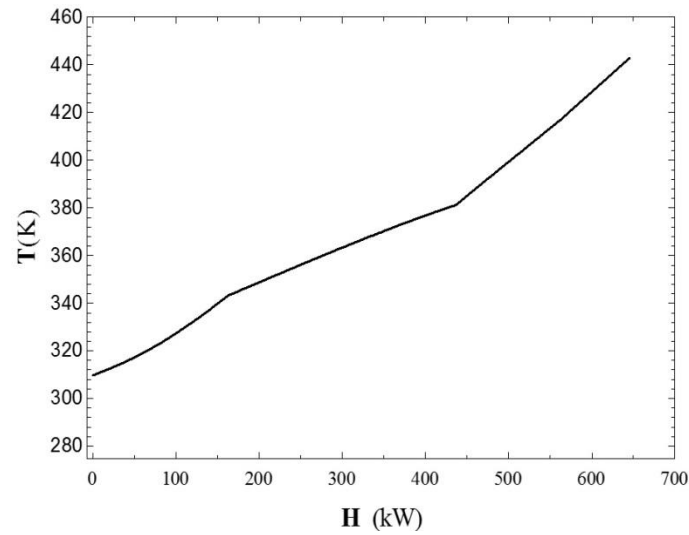
5.Results

In this study, the effect of the heat exchangers’ variation of UAs on the generated power, the cycle thermal efficiency, and the stack exhaust temperature are examined in Table 3. Moreover, the consequences of the cited variations on the pinch-related curves, the composite curve, and the grand composite curve, are observed. The specifications of the studied cycle are shown in Table 1.

The data given in Table 1 are the input data. The simulation results that include all the points (thermodynamic conditions), which are the outcomes of the input data, are summarized in Table 2.



(a)



(b)

Fig.6. Temperature versus enthalpy of (a) the heat exchangers hot streams and (b) the method resulting composite curve

Table 1. The cycle; hot and cold sources specifications.

Specification	Value
1- The hot source	
Components	$y_{CO_2}=0.03, y_{H_2O}=0.07, y_{O_2}=0.15, y_{N_2}=0.75$
Inlet temperature (T_{11})	443K
Mass flow rate (\dot{m}_{11})	3kg/s
2- The cold source	
Components	Water
Mass flow rate (\dot{m}_{13})	1kg/s
Working pressure (P_{13})	1 bar
3- The Kalina cycle	
Main stream ammonia mass fraction (x_1)	0.6
Main stream mass flow rate (\dot{m}_1)	0.24 kg/s
High Pressure of the cycle (P_1)	15.5 bar
4- UA	
Evaporator's UA (UA_{eva})	25 kW/K
Condenser's UA (UA_{con})	15 kW/K
Regenerator's UA (UA_{reg})	2 kW/K

Table 2. Simulation results based on the data given in Table 1

Points	Temperature (K)	Pressure (bar)	Ammonia mass fraction	Vapor fraction	Mass flow rate (kg/s)
1	417.4	15.5	0.6	0.6895	0.24
2	417.4	15.5	0.7736	1	0.1655
3	417.4	15.5	0.2145	0	0.0745
4	386.4	6.925	0.7736	0.9514	0.1655
5	310.7	15.5	0.2145	0	0.0745
6	310.8	6.925	0.2145	0	0.0745
7	381.1	6.925	0.6	0.6148	0.24
8	309.7	6.925	0.6	0	0.24
9	309.8	15.5	0.6	0	0.24
10	339.9	15.5	0.6	0	0.24
11	443.2	1	---	---	3
12	343.2	1	---	---	3
13		288	1	---	1
14	358.2	1	---	---	1

To study the effect of UA variation on decisive parameters including thermal efficiency and the net power output, Table 3 is presented. For a rational justification of the

data given in Table 3, the required explanations are accompanied by those of the temperature–enthalpy curves of each heat exchanger.

Table 3. Decisive parameters of the Kalina cycle for different UAs

Decisive parameters	Base case	Evaporator Variations		Regenerator Variations		Condenser Variations	
		UA=15	UA=35	UA=1	UA=5	UA =10	UA =20
Thermal efficiency	0.07409	0.07744	0.07292	0.07326	0.7424	0.05115	0.0853
Net power output (kW)	23.54	22.88	23.75	23.39	23.57	16.02	27.3
Temperature of the exhaust flue gas(K)	343.2	350.3	340.7	342.7	343.3	344.7	342.5
Condenser pressure(bar)	6.925	6.94	7.005	6.948	6.918	9.067	6.028
Evaporator Pinch temperature difference (K)	3.604	10.34	1.205	3.732	3.61	3.935	3.907
Regenerator Pinch temperature difference (K)	1.245	2.03	1.032	9.131	0.1252	1.062	1.333
Condenser Pinch temperature difference (K)	16.46	15.33	17.02	16.74	16.58	26.56	11.56
Pinch temperature	317.6	315.8	398.1	317.8	317.4	397.9	312.9
Pinch temperature difference (K)	15.36	14.41	14.85	16.2	15.43	16.15	11.27

4.1. Evaporator

In order to analyse the consequences of UA variation of the heat exchangers, the hot and the cold streams' curves are drawn for each of the heat exchangers. As observable in Figure 6, an increment in the evaporator's UA has the greatest influence on the evaporator's temperature–enthalpy curve. Figure 7(a) shows that the pinch temperature falls at the exhaust outlet. As the UA reduces, the heat source exhaust moves upward in a manner in which it changes from 343.2 K to 350.3 K. On the other hand, UA increment to 35 kW/K leads to a temperature reduction to 340.7 K. This temperature reduction is due to the larger amount of heat transfer in the evaporator, which results in more power generation as shown in Table 3. Figure 7(b) shows that when the evaporator heat exchanger's UA shrinks, the heat transfer in the regenerator

improves. As the evaporator's UA reduces, lesser vapour enters the separator; therefore, the mass flow rate of the separator liquid extract diminishes, which results in a better match between the regenerator's streams. As a result, as shown in Table 3, for the evaporator's least UA ($UA=15$ kW/K), the regenerator experiences the largest pinch temperature difference. The faint increase in the power generation as the UA increases is, after all, justified as the cycle efficiency diminishes. Considering Fig. 7(c), it can be seen that the variation in the evaporator's UA does not have a significant effect on the condenser's stream curves. Figure 8(a) demonstrates that an increase in UA raises the pinch temperature difference up to 81 °C. As observable in Fig.8(b), the UA reduction causes a comparatively large packet above the pinch point, which proposes an integration above the pinch point.

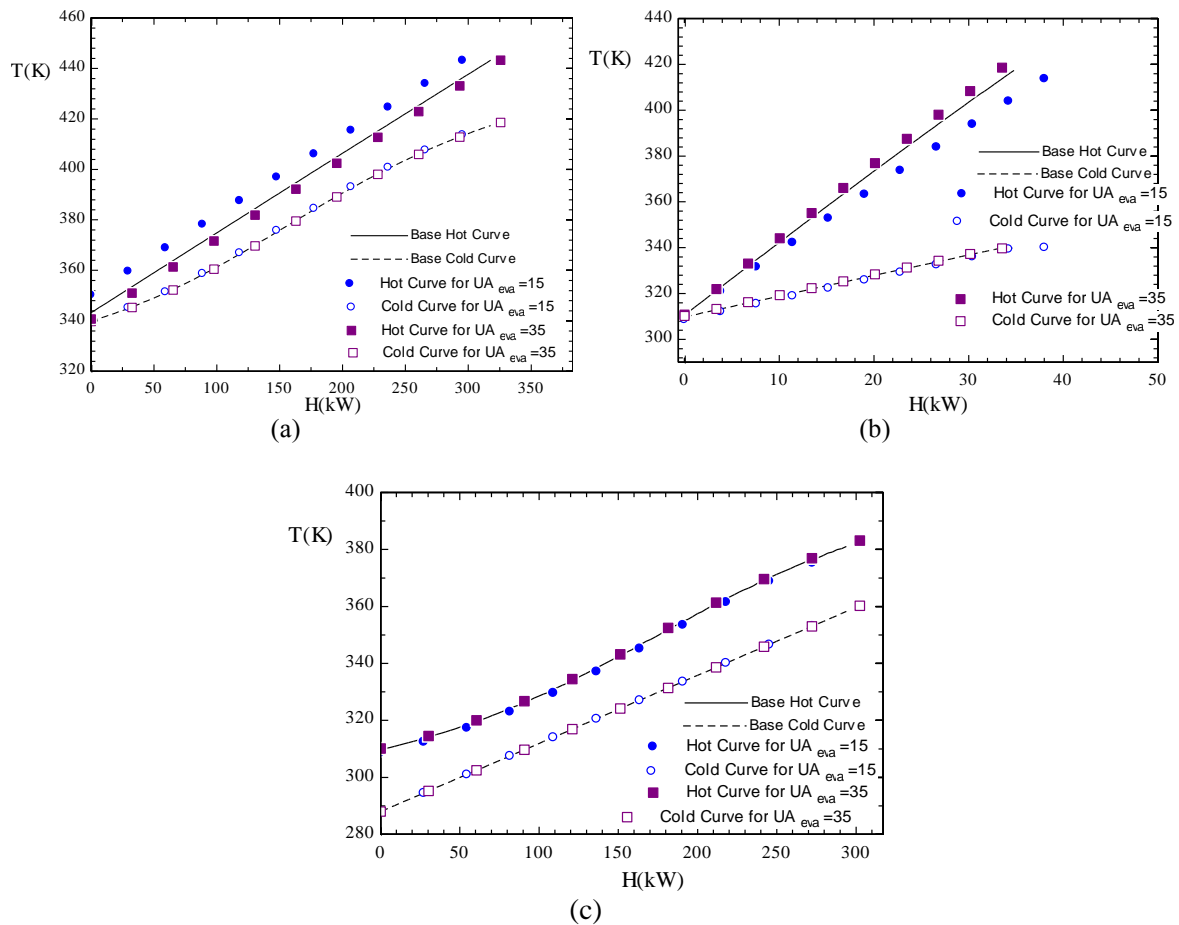


Fig.7. Temperature variation versus enthalpy as the evaporator UA varies for (a) the evaporator, (b) the regenerator, and (c) the condenser.

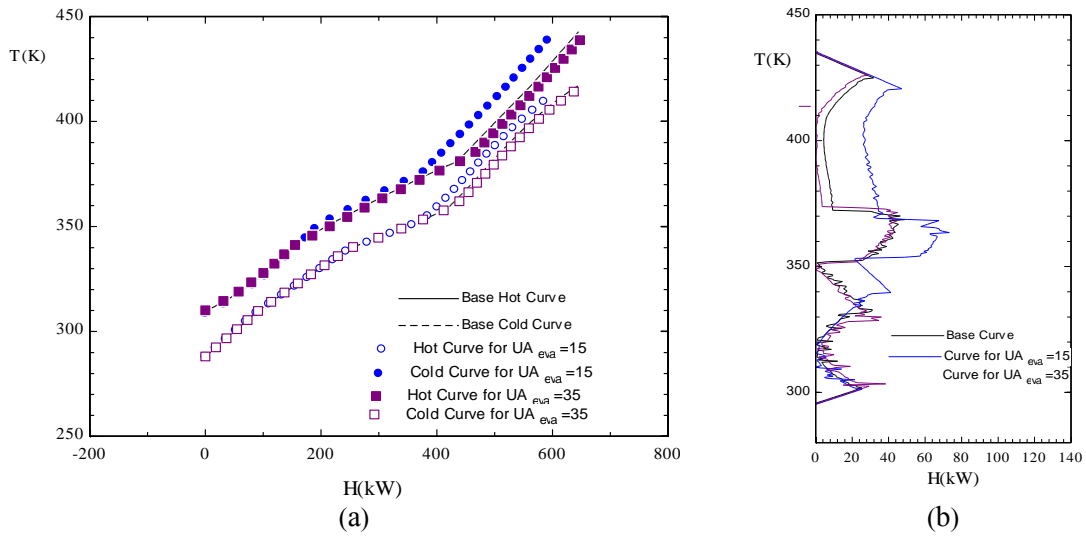


Fig.8. Pinch related curves for the three evaporator UAs: (a) composite curve and (b) grand composite curve

4.2. Regenerator

Figure 9 shows the effect of the regenerator's UAs on the stream curves of the heat exchangers. As observable in the figures, the

regenerator's UA variation negligibly affects the heat exchangers' stream curves. The maximum changes are, however, observable for the heat exchanger's stream curves. A change in the regenerator's UA does not

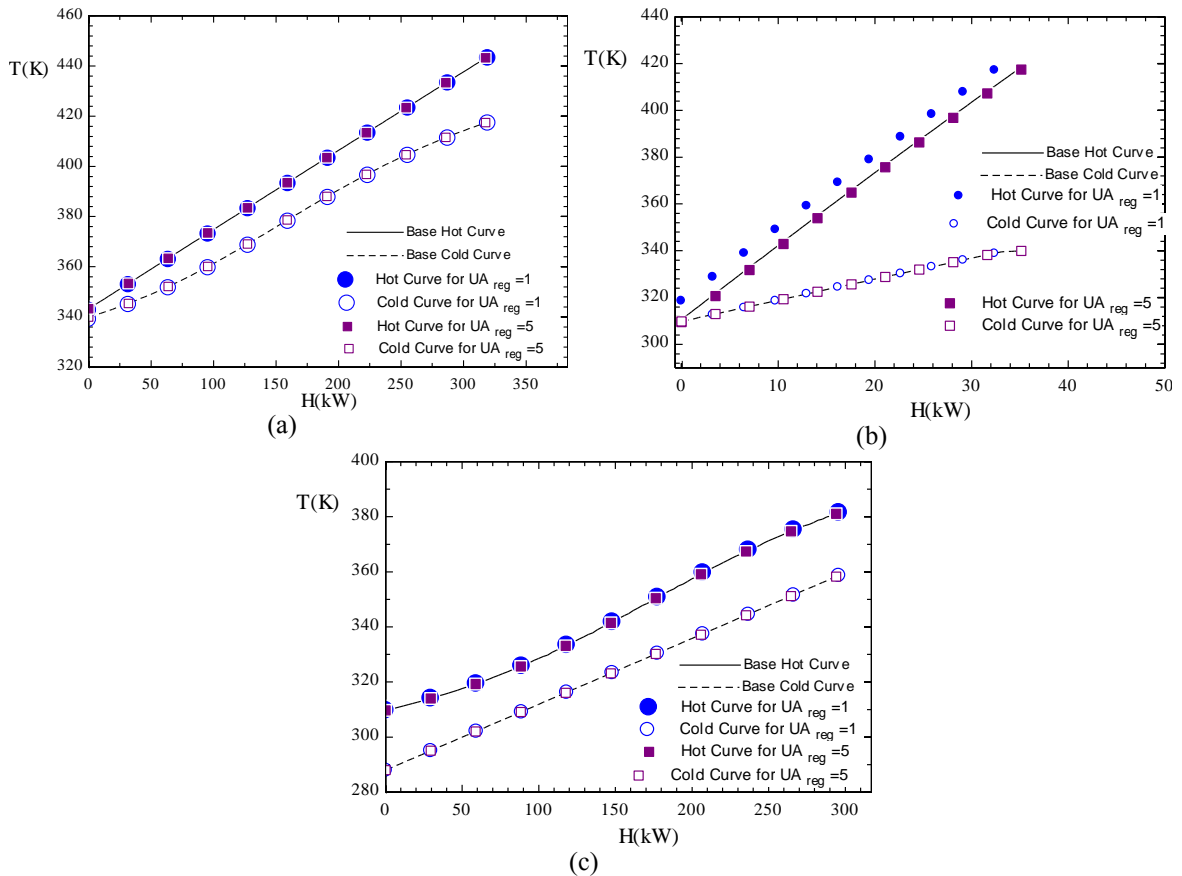


Fig.9. Temperature variation versus enthalpy as the regenerator UA varies for (a) the evaporator, (b) the regenerator, and (c) the condenser

affect the stream curves; this is a result of the large difference between the slopes of the two curves in this component. This difference restricts the feasibility of a promoted heat recovery when the heat exchanger's area expands. According to Fig.10, therefore, both the composite curve and the grand composite curve are not subjected to a considerable deformation for the three UAs. The effect of the heat transfer reduction, however, in comparison with the increase of the UAs, seems to be greater, which is also confirmed by Table 3. In other words, as the regenerator's UA reduces 1, the regenerator pinch temperature difference increases to about 10°C. In reverse, as the UA reaches 5kW/K, the temperature difference reduces to about 0.8°C.

4.3. Condenser

According to Table 3, among the heat transfer variations, only the condenser's UA increase leads to 66 percent improvement in the

cycle's efficiency and a 70 percent increase in the generated power. As observable in Fig. 11, these improvements are due to an appropriate match between the hot and the cold streams in the heat exchanger, which results in perfect heat recovery and the turbine's back-pressure reduction. In other words, increasing the heat exchanger's UA to 20kW/K, causes the turbine's back-pressure to approach 6 bar, which is the least value in Table 3. As a result, the net power output is surprisingly subjected to a 4 kW increase. Considering the other heat exchangers' streams curves, it can be concluded that the condenser's UA variation affects the evaporator's stream curves less intensely. As observable in Fig.12, the condenser's UA reduction results in an increase in the pinch temperature; this shrinks the previously existing packet above the pinch point. No integration, therefore, seems to be available after the UA reduction there. On the other hand, a large gap below the pinch temperature may be a hint for integration there.

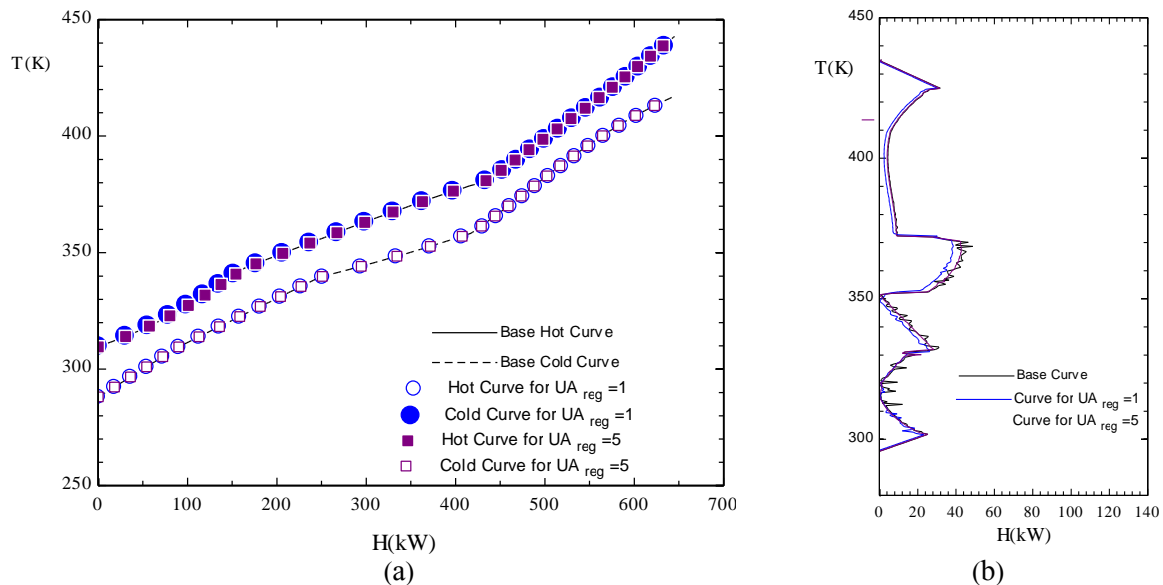


Fig.10. Pinch related curves for the three regenerator UAs: (a) composite curve and (b) grand composite curve

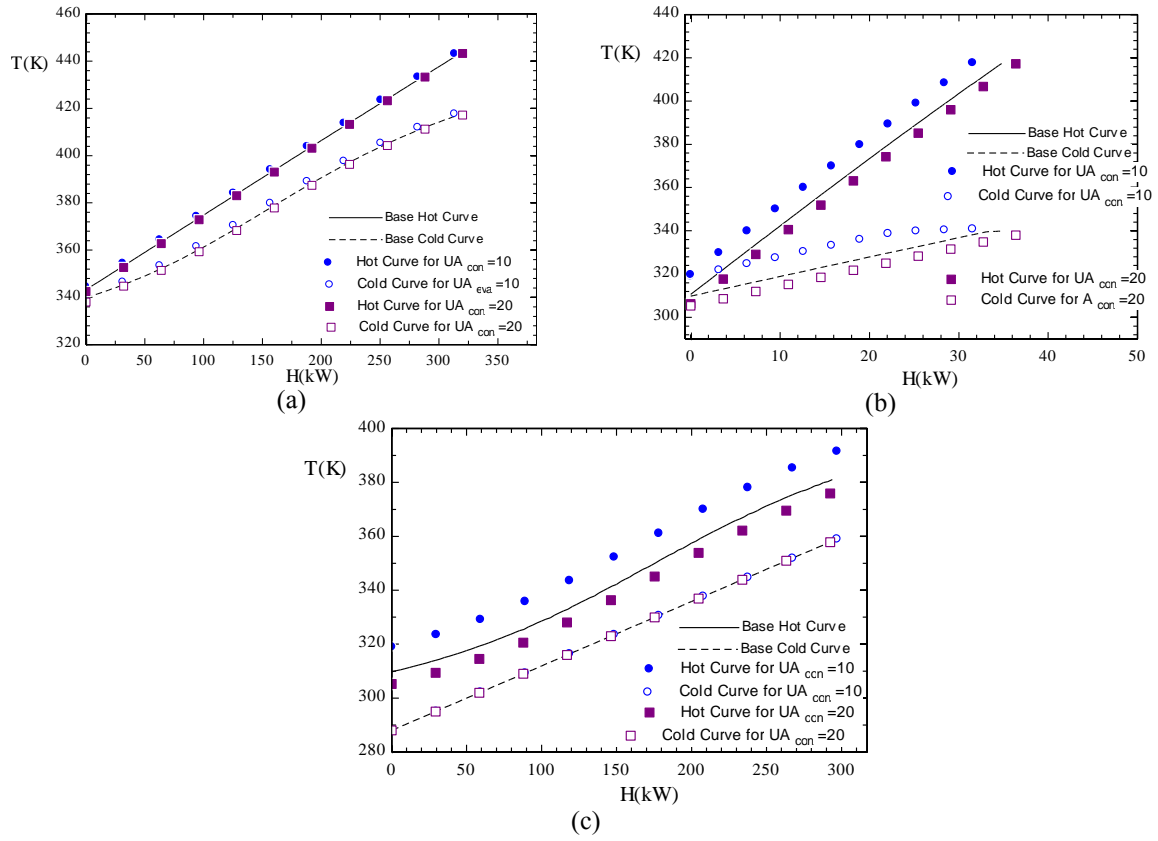


Fig.11. Temperature variation versus enthalpy as the condenser UA varies for (a) the evaporator, (b) the regenerator, and (c) the condenser

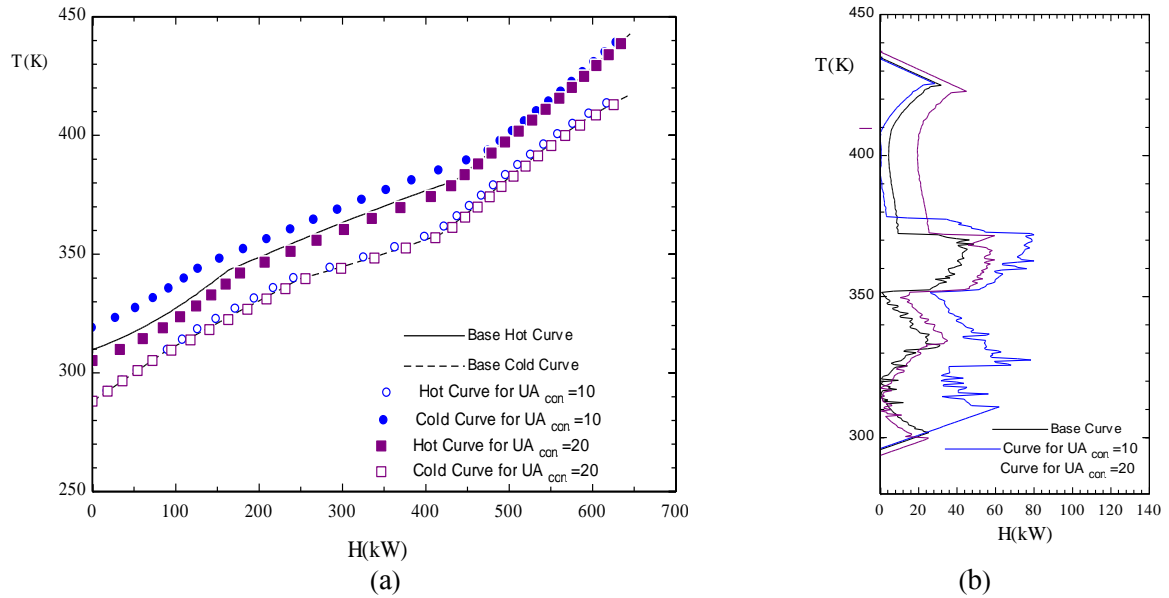


Fig.12. Pinch-related composite curves for the three condenser UAs: (a) composite curve and (b) grand composite curve

5. Conclusion

In this paper, the effect of the product of the overall heat transfer coefficient and the area in the KCS 11 heat exchanger is examined. The non-linear behaviour of the water–ammonia mixture during the phase transition necessitates the implementation of the finite difference method. By analysing each of the stream curves for the heat exchangers while composite curve and the grand composite curve are drawn, the following deductions are made:

- Although an increase in the evaporator UA increases the amount of generated power, it diminishes the cycle's efficiency, which is due to the change in the mass flow rate of the liquid extract of the separator and the intensified mismatch in the streams' heat capacities.
- Varying the regenerator's UA does not have a significant effect on the thermal conditions of the cycle, which can be explained by the difference between the hot and the cold streams' heat capacity in this heat exchanger.
- The most effective variation is related to the condenser's UA. In fact, an increase from 15kW/K to 20 kW/K increases both, the cycle's efficiency and the power output, by about 70 percent.

References

- [1] Kalina A.I., Combined-Cycle System with Novel Bottoming Cycle, *Journal of Engineering for Gas Turbines and Power*, (1984)106(4): 737-742.
- [2] Madhawa Hettiarachchi H. D., Golubovic M., Worek, and Y. Ikegami W. M., The Performance of the Kalina Cycle System 11(KCS-11) with Low-Temperature Heat Sources, *Journal of Energy Resources Technology* (2007)129(3): 243-247.
- [3] Zhang X., He M., Zhang Y., A Review of Research on the Kalina Cycle, *Renewable and Sustainable Energy Reviews* (2012) 16(7): 5309-5318.
- [4] Li X., Zhang Q., Li X., A Kalina Cycle with Ejector, *Energy* (2013)54: 212-219.
- [5] He J., Liu C., Xu X., Li Y., Wu S., and Xu J., Performance Research on Modified KCS (Kalina cycle system) 11 without Throttle Valve, *Energy* (2014)64: 389-397.
- [6] Yue C., Han D., Pu W., and He W., Comparative Analysis of a Bottoming Transcritical ORC and a Kalina Cycle for Engine Exhaust Heat Recovery, *Energy Conversion and Management* (2015) 89(0): 764-774.
- [7] Yari M., Mehr A. S., Zare V., Mahmoudi S. M. S., Rosen M. A., Exergoeconomic Comparison of TLC (Trilateral Rankine Cycle), ORC (Organic Rankine Cycle) and Kalina Cycle Using a Low Grade Heat Source, *Energy* (2015)83: 712-722.
- [8] Mlcak H., Kalina Cycle Concepts for Low Temperature Geothermal, *Geothermal Resources in Geothermal Resources Council Transactions* (2002) 707-713.
- [9] Sun F., Ikegami Y., Jia B., A Study on Kalina Solar System with an Auxiliary Superheater, *Renewable Energy* (2012) 41: 210-219.
- [10] Wang J., Yan Z., Zhou E., and Dai Y., Parametric Analysis and Optimization of a Kalina Cycle Driven by Solar Energy. *Applied Thermal Engineering* (2013)50(1):408-415.
- [11] Ogriseck S., Integration of Kalina Cycle in a Combined Heat and Power Plant, A Case Study, *Applied Thermal Engineering* (2009) 29(14–15): 2843-2848.
- [12] Singh O.K., Kaushik S.C., Energy and Exergy Analysis and Optimization of Kalina Cycle Coupled with a Coal Fired Steam Power Plant, *Applied Thermal Engineering* (2013)51(1–2): 787-800.
- [13] Bram S., De Ruyck J., Exergy Analysis and Design of Mixed CO₂/Steam Gas Turbine Cycles, *Energy Conversion and Management* (1995)36(6–9): 845-848.
- [14] Anantharaman R., Abbas O.S., Gundersen T., Energy Level Composite Curves—A New Graphical Methodology for the Integration of Energy Intensive Processes, *Applied Thermal Engineering*, (2006) 26(13): 1378-1384.
- [15] Esen H., Inalli M., Esen M., and Pihtili K., Energy and Exergy Analysis of a Ground-Coupled Heat Pump System with Two Horizontal Ground Heat Exchangers, *Building and Environment*, (2007) 42(10): 3606-3615.
- [16] Ghaebi H., Amidpour M., Karimkashi S., and Rezayan O., Energy, Exergy and Thermoeconomic Analysis of a Combined Cooling, Heating and Power (CCHP) System with Gas Turbine Prime Mover, *International Journal of Energy Research*, (2011)35(8): 697-709.

- [17]Arriola-Medellín A., Manzanares-Papayanopoulos E., Romo-Millares C., Diagnosis and Redesign of Power Plants Using Combined Pinch and Exergy Analysis, *Energy* (2014)72(0): 643-651.
- [18]Kim K.H., Ko H.J., Kim K., Assessment of Pinch Point Characteristics in Heat Exchangers and Condensers of Ammonia–Water Based Power Cycles, *Applied Energy* (2014)113(0): 970-981.
- [19]Schaefer L.A., Heat Exchanger Mean Temperature Differences for Refrigerant Mixtures, in *Mechanical Engineering*, Georgia Institute of Technology (1997)
- [20]Linnhoff B., Sahdev V., Pinch Technology, in *Ullmann's Encyclopedia of Industrial Chemistry*, Wiley-VCH Verlag GmbH and Company KGaA (2000).
- [21]Steam and Power Systems, in *Industrial Boilers and Heat Recovery Steam Generators*, CRC Press (2002).
- [22]Ibrahim O.M., Klein S.A., Thermodynamic Properties of Ammonia-Water Mixtures, *ASHRAE Transactions* (1993)1495-1502.